

Electronic Structure of the PYP Chromophore in Its Native Protein Environment

Evgeniy V. Gromov,^{*,†,‡} Irene Burghardt,^{*,§} Horst Köppel,[†] and Lorenz S. Cederbaum[†]

Contribution from the Theoretische Chemie, Physikalisch-Chemisches Institut Universität Heidelberg, Im Neuenheimer Feld 229, D-69120 Heidelberg, Germany, Laboratory of Quantum Chemistry, Computer Center, Irkutsk State University, K. Marks 1, 664003 Irkutsk, Russian Federation, and Département de Chimie, Ecole Normale Supérieure, 24 rue Lhomond, F-75231 Paris cedex 05, France

Received December 21, 2006; E-mail: evgeniy.gromov@pci.uni-heidelberg.de; irene.burghardt@ens.fr

Abstract: We report on supermolecular ab initio calculations which clarify the role of the local amino acid environment in determining the unique electronic structure properties of the photoactive yellow protein (PYP) chromophore. The extensive ab initio calculations, at the level of the CC2 and EOM-CCSD methods, allow us to explicitly address how the interactions between the deprotonated *p*-coumaric thio-methyl ester (*p*CTM⁻) chromophore and the surrounding amino acids act together to create a specifically stabilized *p*CTM⁻ species. Particularly noteworthy is the role of the Arg52 amino acid in stabilizing the chromophore against autoionization, and the role of the Tyr42 and Glu46 amino acids in determining the hydrogen-bonding properties that carry the dominant energetic effects.

I. Introduction

The majority of living organisms possess the ability to perceive light and exploit it for biological function. Among the most striking examples are photosynthesis and vision. Another, less known, functionality derived from the interaction with light relates to *photomotility*, i.e., light-induced motion, which plays a vital role for various microorganisms.¹ Here, a light-induced signal is transduced to the motor apparatus so as to make the microorganism navigate to an environment which is more or less strongly illuminated (positive vs negative phototaxis). An intriguing fact is that the very initial photoresponse, at a molecular level, often relates to a photoisomerization mechanism—very similarly to retinal photoisomerization in the visual process.

The present study addresses the primary steps in the photoresponse of the *Halorhodospira halophila* bacterium, which exhibits a negative phototactic response when irradiated with blue light.² The photoreceptor mediating this response is the photoactive yellow protein (PYP),³ a small protein (14 kDa) comprising 125 amino acids and a unique cofactor—the anionic *p*-hydroxycinnamoyl chromophore (also referred to as a *p*-coumaric thio ester derivative in the following). PYP undergoes a photocycle which is initiated by the isomerization of the chromophore's double bond, on a subpicosecond time scale. The overall photocycle extends over a time scale of seconds,

and involves the protonation of the chromophore (on a microsecond time scale) as well as the partial unfolding of the protein (on a millisecond time scale).

PYP has been studied extensively over the past few years, both experimentally and theoretically (see the recent reviews^{4–9}). Recent theoretical studies include, in particular, various efforts at identifying the photoisomerization mechanism^{10–15} and the role of the protein in triggering the isomerization.^{15–17}

Despite these efforts, many open questions remain. This concerns, in particular, the highly specific influence exerted by the local amino acid environment on the anionic chromophore. In the work reported here, we therefore aim to obtain a highly accurate ab initio picture of the supermolecular complex

[†] Physikalisch-Chemisches Institut Universität Heidelberg.

[‡] Irkutsk State University.

[§] Ecole Normale Supérieure.

(1) Sgarbossa, A.; Checcucci, G.; Lenci, F. *Photochem. Photobiol. Sci.* **2002**, *1*, 459.

(2) Meyer, T. E. *Biochim. Biophys. Acta* **1985**, *806*, 175.

(3) Sprenger, W. W.; Hoff, W. D.; Armitage, J. P.; Hellingwerf, K. J. *J. Bacteriol.* **1993**, *175*, 3096.

(4) Hellingwerf, K. J.; Hendriks, J.; Gensch, T. *J. Phys. Chem. A* **2003**, *107*, 1082.

(5) Hellingwerf, K. J.; Hendriks, J.; Van Der Horst, M.; Haker, A.; Crielaard, W.; Gensch, T. *Compr. Ser. Photochem. Photobiol.* **2003**, *3*, 228.

(6) Hendriks, J.; Hellingwerf, K. J. In *CRC Handbook of Organic Photochemistry and Photobiology*, 2nd ed.; Horspool, W. M., Lenci, F., Eds.; CRC Press LLC: Boca Raton, FL, 2004.

(7) Vreede, J.; Van Der Horst, M. A.; Kort, R.; Crielaard, W.; Hellingwerf, K. J. *Phase Transitions* **2004**, *77*, 3.

(8) Changenet-Barret, P.; Espagne, A.; Plaza, P.; Hellingwerf, K. J.; Martin, M. M. *New J. Chem.* **2005**, *29*, 527.

(9) Larsen, D. S.; van Grondelle, R. *ChemPhysChem* **2005**, *6*, 828.

(10) Yamada, A.; Yamamoto, S.; Yamato, T.; Kakitani, T. *J. Mol. Struct. (Theochem)* **2001**, *536*, 195.

(11) Antes, I.; Thiel, W.; van Gunsteren, W. F. *Eur. Biophys. J.* **2002**, *31*, 504.

(12) Groenhof, G.; Lensink, M. F.; Berendsen, H. J. C.; Snijders, J. G.; Mark, A. E. *Proteins* **2002**, *48*, 202.

(13) Groenhof, G.; Lensink, M. F.; Berendsen, H. J. C.; Mark, A. E. *Proteins* **2002**, *48*, 212.

(14) Thompson, M. J.; Bashford, D.; Noodleman, L.; Getzoff, E. D. *J. Am. Chem. Soc.* **2003**, *125*, 8186.

(15) Groenhof, G.; Bouxin-Cademartory, M.; Hess, B.; de Visser, S. P.; Berendsen, H. J. C.; Olivucci, M.; Mark, A. E.; Robb, M. A. *J. Am. Chem. Soc.* **2004**, *126*, 4228.

(16) Yamada, A.; Ishikura, T.; Yamato, T. *Proteins* **2004**, *55*, 1063.

(17) Yamada, A.; Ishikura, T.; Yamato, T. *Proteins* **2004**, *55*, 1070.

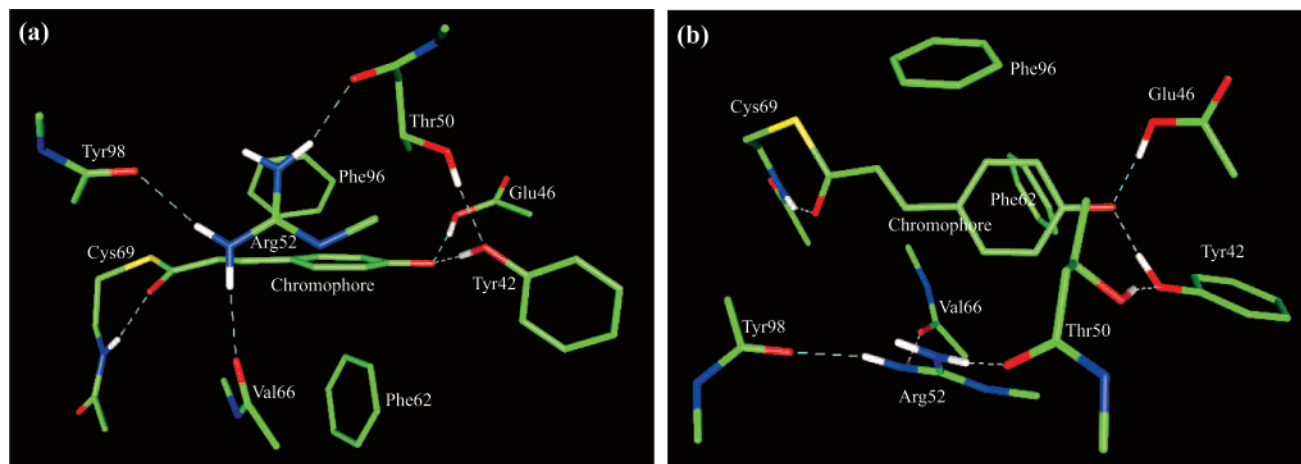


Figure 1. Supermolecular complex containing the PYP chromophore and nine surrounding amino acids: (a) side view; (b) top view. Only the hydrogen atoms involved in hydrogen bonding are shown.

constituted by the chromophore and the amino acids in its immediate neighborhood. To identify the specific influence of the individual amino acids, we construct a series of such supermolecular systems of increasing size and compare their properties. Key results include that (i) the positively charged Arg52 residue mainly stabilizes the deprotonated chromophore against autoionization but does not have a strong effect on the energetics and (ii) the Tyr42 and Glu46 amino acids, which are connected to the chromophore by hydrogen bonds, exert the most pronounced effect on the energy ordering. These conclusions prepare the ground for obtaining a precise description of the isomerization process in the native protein.

All complexes were calculated using pure ab initio methods, in particular the second-order approximate coupled cluster singles and doubles (CC2) method, and, where possible, the more accurate equation-of-motion coupled-cluster singles and doubles (EOM-CCSD) method. The good accuracy of the CC2 method, in conjunction with its moderate computational cost, makes it one of today's most efficient tools in the study of relatively large molecular systems. In the present study, this method is applied to remarkably large and complex molecular objects—comprising more than 100 atoms. This paves the way toward future large-scale electronic structure calculations.

A complementary investigation, also reported below, concerns the anionic nature of the chromophore, as compared with the protonated form. This study complements our previous investigation¹⁸ of the protonated species. Importantly, the π - π^* state which is involved in the isomerization process is the lowest-lying excited state in the anionic chromophore, which is not the case for the protonated chromophore. In the amino acid environment, the chromophore will be seen to essentially retain the electronic structure characteristics of the anion.

The paper is organized as follows. In section II, we give details of the calculational procedures. In section III, we present and analyze our results and give a comparison with experimental data. Section IV summarizes and concludes.

II. Computational Details

A series of supermolecular chromophore-amino acid complexes were constructed, using the atomic coordinates of PYP determined in the recent X-ray crystallographic study of ref 19. The largest complex,

comprising the chromophore and 9 amino acid fragments (Figure 1) was constructed first, as a reference for all other calculations. The relevant amino acids were cut at C–C bonds, taking the most important molecular fragments closely lying to the chromophore (peptide bonds, hydrogen-bonded atoms) into account. Free valences of the cutoff carbons were capped with hydrogens. The positions of all hydrogen atoms in the complex were fully optimized using the HF method and the 6-31G* basis set. The selected amino acids represent the complete nearest-neighbor environment of the chromophore, located at about 3 Å from the “chromophore's center”. To identify the effects exerted by particular amino acids, several reduced complexes were constructed, by removing chosen amino acid fragment(s) from the original complex.

The isolated neutral and anionic species of the chromophore were obtained by removing all environmental amino acids, with the Cys69 fragment being replaced by a thio-methyl group. In the case of the neutral isolated chromophore, an additional hydrogen atom was added to the phenolic oxygen of the anionic species, and a full optimization of its position was carried out. Coordinates of all molecular systems considered in this work can be found in the Supporting Information.

To calculate the vertical transition energies and electronic structure properties of the excited states of the various complexes, we made use of the second-order approximate coupled-cluster singles and doubles (CC2) method.²⁰ For the smaller complexes, the more accurate equation-of-motion coupled-cluster singles and doubles (EOM-CCSD) method^{21–23} was used. By employing the resolution-of-the-identity (RI-CC2) approximation^{24–26} in the CC2 calculations, results for very large complexes, comprising up to about hundred atoms, could be obtained. The CC2 method gives quite good results (with typical errors within the 0.3–0.5 eV range) if the excited-state electronic structure is dominated by single electron excitations. The EOM-CCSD method is more sophisticated and more accurate than the CC2 method. The average accuracy of the EOM-CCSD scheme is generally considered to be of 0.2–0.4 eV^{27,28} for excited states with a not too high (less

(18) Gromov, E. V.; Burghardt, I.; Köppel, H.; Cederbaum, L. S. *J. Phys. Chem. A* **2005**, *109*, 4623.

(19) Kort, R.; Hellingwerf, K. J.; Ravelli, R. B. G. *J. Biol. Chem.* **2004**, *279*, 26417.
 (20) Christiansen, O.; Koch, H.; Jørgensen, P. *Chem. Phys. Lett.* **1995**, *243*, 409.
 (21) Sekino, H.; Bartlett, R. J. *Int. J. Quantum Chem. Quantum Chem. Symp.* **1984**, *18*, 255.
 (22) Geertsen, J.; Rittby, M.; Bartlett, R. J. *Chem. Phys. Lett.* **1989**, *164*, 57.
 (23) Stanton, J. F.; Bartlett, R. J. *J. Chem. Phys.* **1993**, *98*, 7029.
 (24) Vahtras, O.; Almlöf, J.; Feyereisen, M. W. *Chem. Phys. Lett.* **1993**, *213*, 514.
 (25) Eichkorn, K.; Treutler, O.; Öhm, H.; Häser, M.; Ahlrichs, R. *Chem. Phys. Lett.* **1995**, *240*, 283.
 (26) Ahlrichs, R. *Phys. Chem. Chem. Phys.* **2004**, *6*, 5119.
 (27) Koch, H.; Christiansen, O.; Jørgensen, P.; Olsen, J. *Chem. Phys. Lett.* **1995**, *244*, 75.
 (28) Christiansen, O.; Koch, H.; Jørgensen, P.; Olsen, J. *Chem. Phys. Lett.* **1996**, *256*, 185.

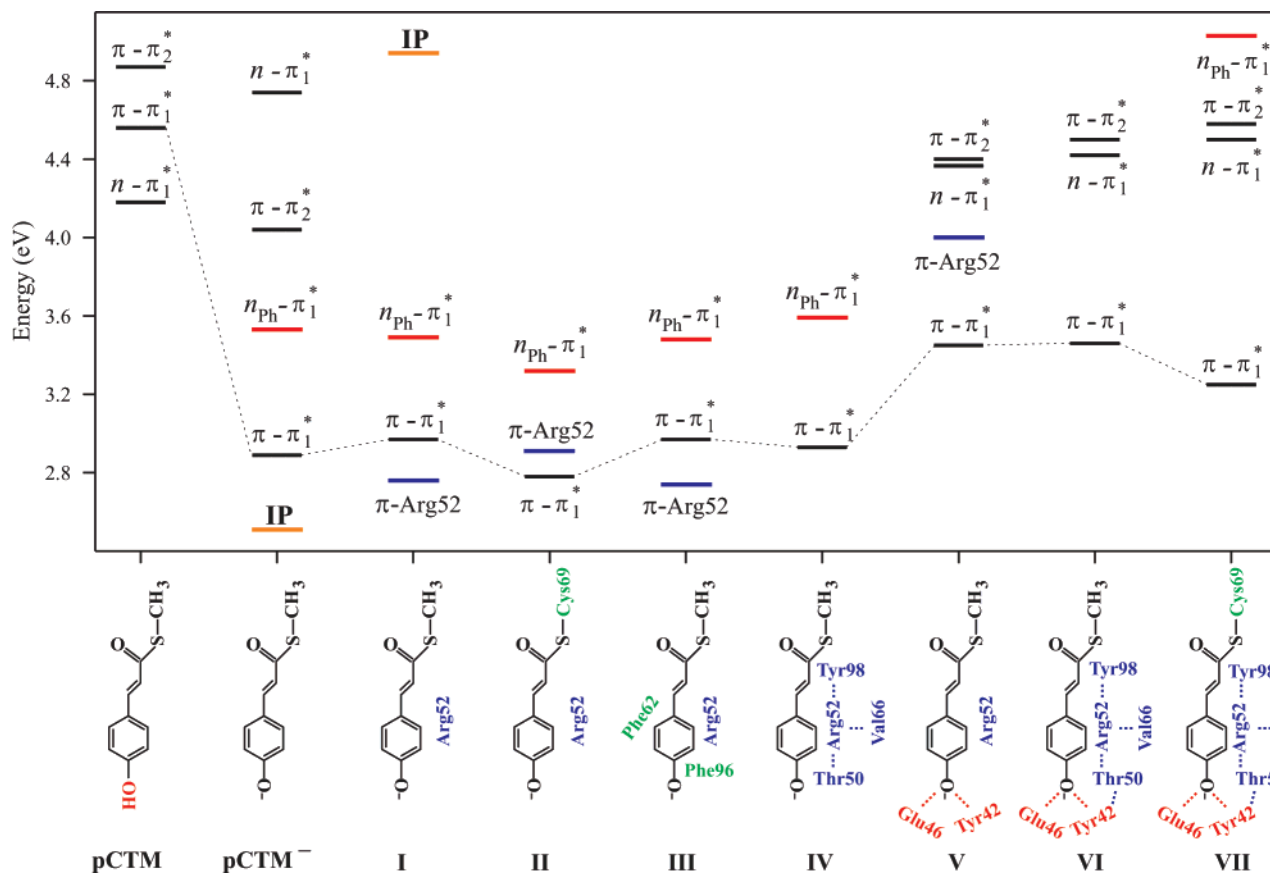


Figure 2. Diagram of vertical transition energies for the low-lying excited singlet states of the different molecular systems and supermolecular complexes under consideration. The results have been obtained with the CC2 method and the SV(P) basis set. The transition energy of the $n_{\text{ph}}-\pi_1^*$ state was shifted up by 0.69 eV (see section III for details). Note that our present findings for the neutral *p*CTM chromophore suggest an inversion of the $\pi-\pi_1^*$ and $\pi-\pi_2^*$ excited states as compared with the state ordering reported in our previous work.¹⁸ (The $\pi-\pi_1^*$ and $\pi-\pi_2^*$ states correspond to the $^1A'(V)$ and $^1A''(V)$ states of ref 18). This change in the state ordering is due to differences in the molecular geometry and strong mixing between the $\pi-\pi_1^*$ and $\pi-\pi_2^*$ states.

than 20%) weight of doubly excited configurations. In the present work, the results of EOM-CCSD calculations have been used systematically to test and calibrate the CC2 method.

The SV(P)²⁹ and 6-31G*^{30–32} double- ζ plus polarization basis sets were used in all CC2 and EOM-CCSD calculations. Diffuse functions were found to have a minor influence on the excited states localized on the chromophore, resulting in an almost uniform red shift by about 0.2 eV (see discussion in the Supporting Information). A much more pronounced lowering, of about 0.8 eV, is observed for the excited states localized on the Arg52 amino acid (see Supporting Information). However, this does not affect our results and conclusions, since we are focusing on relative changes of excitation energies, and, more importantly, the states in question are not relevant for the larger complexes addressed below.

Our CC2 calculations were performed using the TURBOMOLE program suite,³³ while for the EOM-CCSD calculations the ACES II program package was employed.³⁴ In all coupled-cluster calculations, the core MOs were kept frozen.

We will also be interested in the first ionization potential (IP) of the systems under consideration. This quantity was evaluated using the outer-valence Green's function (OVGF) method.³⁵ The IP was found to be sensitive to the presence of diffuse functions in the basis set

(ignoring diffuse functions results in an IP lying about 0.5 eV lower). Therefore the 6-31+G* basis set,^{30–32} containing diffuse functions on second row atoms, was used in the OVGF calculations. The latter were performed with the Gaussian suite of programs.³⁶

III. Results and Discussion

Figure 2 summarizes our main results, in terms of transition energies of the relevant low-lying excited singlet states of the nine molecular systems under consideration (the explicit values of the transition energies are given in the Supporting Information, Table SM2). The first and second systems are the neutral versus anionic (deprotonated) *p*-coumaric thio-methyl ester chromophores in the absence of the amino acid environment. These are denoted *p*CTM and *p*CTM[−], respectively. All other molecular systems, referred to by roman numerals I to VII (see Figure 2), are supermolecular complexes obtained by adding certain amino acid fragments to the *p*CTM[−] chromophore. System VII is the largest complex and represents the native protein environment (Figure 1), except that the Phe62 and Phe96 amino acid fragments have been disregarded. (It is shown below that Phe62 and Phe96 have little effect on the excited states).

For each of the systems under consideration, the vertical transition energies of the relevant low-lying excited singlet states

(29) Schaefer, A.; Horn, H.; Ahlrichs, R. *J. Chem. Phys.* **1992**, *97*, 2571.

(30) Hehre, W. J.; Ditchfield, R.; Pople, J. A. *J. Chem. Phys.* **1972**, *56*, 2257.

(31) Hariharan, P. C.; Pople, J. A. *Theor. Chem. Acc.* **1973**, *28*, 213.

(32) Francl, M. M.; Pietro, W. J.; Hehre, W. J.; Binkley, J. S.; Gordon, M. S.; DeFrees, D. J.; Pople, J. A. *J. Chem. Phys.* **1982**, *77*, 3654.

(33) Ahlrichs, R.; Bär, M.; Häser, M.; Horn, H.; Kölmel, C. *Chem. Phys. Lett.* **1989**, *162*, 165.

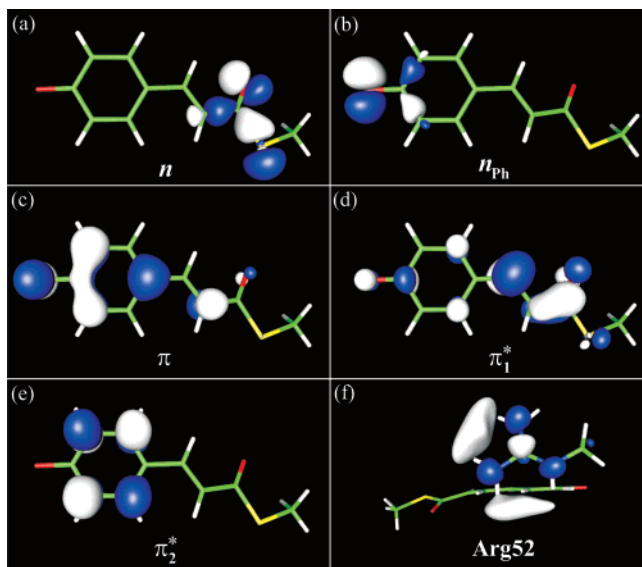
(34) Stanton, J. F.; et al. *ACES II*, Mainz-Austin-Budapest Version; <http://www.aces2.de>.

(35) von Niessen, W.; Schirmer, J.; Cederbaum, L. S. *Comput. Phys. Rep.* **1984**, *1*, 57.

(36) Frisch, M. J.; et al. *Gaussian 03*, revision C.02; Gaussian, Inc.: Wallingford, CT, 2004.

Table 1. CC2 Calculated Properties for the $\pi-\pi_1^*$, $\pi-\pi_2^*$, $n-\pi_1^*$, $n_{\text{Ph}}-\pi_1^*$, and π -Arg52 Excited States in the Different Chromophore + Amino Acid(s) Supermolecular Complexes: Oscillator Strengths, f (au); Change in the Permanent Dipole Moment under Transition to the Excited State, $|\Delta\vec{\mu}|$ (Debye)

| molecular system/complex | $\pi-\pi_1^*$ | | $\pi-\pi_2^*$ | | $n-\pi_1^*$ | | $n_{\text{Ph}}-\pi_1^*$ | | π -Arg52 | |
|--|---------------|---------------------|---------------|---------------------|-------------------|---------------------|-------------------------|---------------------|--------------|---------------------|
| | f | $ \Delta\vec{\mu} $ | f | $ \Delta\vec{\mu} $ | f | $ \Delta\vec{\mu} $ | f | $ \Delta\vec{\mu} $ | f | $ \Delta\vec{\mu} $ |
| <i>p</i> CTM | 0.867 | 5.8 | 0.099 | 0.7 | 0.011 | 5.6 | | | | |
| <i>p</i> CTM [−] | 0.995 | 7.5 | 0.056 | 0.6 | <10 ^{−3} | 5.7 | 0.015 | 14.7 | | |
| I <i>p</i> CTM [−] + Arg52 | 0.759 | 8.6 | | | | | <10 ^{−3} | 14.1 | 0.053 | 18.6 |
| II I + Cys69 | 0.924 | 6.9 | | | | | 0.003 | 14.9 | 0.107 | 17.8 |
| III I + Phe62 + Phe96 | 0.338 | 12.7 | | | | | <10 ^{−3} | 13.9 | 0.052 | 18.2 |
| IV I + Thr50 + Val66 + Tyr98 | 0.559 | 10.9 | | | | | 0.347 | 12.5 | | |
| V I + Tyr42 + Glu46 | 1.074 | 11.0 | | | | | | | | |
| VI IV + Tyr42 + Glu46 | 1.012 | 11.2 | | | | | | | | |
| VII VI + Cys69 | 1.073 | 11.6 | | | | | | | | |

**Figure 3.** (a–e) Patterns of the principal highest occupied and lowest unoccupied (virtual) molecular orbitals of the deprotonated chromophore (*p*CTM[−]); (f) pattern of the lowest unoccupied molecular orbital of complex I (*p*CTM[−] + Arg52). Note that the orbital patterns of the π and π_1^* orbitals differ from those of the neutral chromophore (see Figure 1 of ref 18). In particular, the π_1^* orbital is no longer localized on the double bond conjugated with the aromatic ring.

are given. The ground states of the respective systems are fixed at zero energy. For *p*CTM[−] and complex I, we also indicate the value of the first ionization potential (IP).

A detailed discussion of the results illustrated in Figure 2 will be given in the following sections. Complementary information is available in Table 1, where we present excited-state one-electron properties, such as oscillator strengths and relative changes of the dipole moment.

The excited states listed in Figure 2 and Table 1 are labeled according to their leading electronic configurations. For each excited state, the relevant configuration corresponds to the promotion of an electron from a high-lying occupied molecular orbital (MO) to a low-lying unoccupied (virtual) MO. The patterns of these MOs are shown in Figure 3 (a–f). They include the occupied n_{Ph} , n , π , and virtual π_1^* , π_2^* MOs (Figure 3a–e), which reside on the chromophore and are present in all systems under consideration. In addition, there is the virtual MO “Arg52” (Figure 3f), which appears only when the Arg52 amino acid fragment is taken into account and which is localized on this fragment. The π MO is always the highest occupied MO (HOMO) while the positions of the other MOs under consid-

eration depend on the chromophore’s environment. The n and n_{Ph} MOs essentially correspond to lone pairs, with the n orbital relating to the carbonyl oxygen lone pair with a contribution from the 3p atomic orbitals of sulfur, while the n_{Ph} orbital corresponds to the lone pair of the phenolic oxygen.

The results presented in the diagram were obtained throughout from CC2 calculations. For *p*CTM, *p*CTM[−], and complex I, we also carried out EOM-CCSD calculations. This allowed us to assess the quality of the CC2 method in describing the excited states under consideration. A comparison of the CC2 and EOM-CCSD data obtained for those three systems shows that the CC2 method correctly describes the $\pi-\pi_1^*$, $\pi-\pi_2^*$, $n-\pi_1^*$, and π -Arg52 excited states, with deviations from the EOM-CCSD energies that are not larger than about 0.3 eV for the $\pi-\pi_1^*$ and $\pi-\pi_2^*$ states, 0.1 eV for the $n-\pi_1^*$ state, and 0.4 eV for the π -Arg52 state. The EOM-CCSD energies are always higher than the CC2 values (explicit values of the excitation energies under consideration can be found in table SM2 of the Supporting Information).

The $n_{\text{Ph}}-\pi_1^*$ excited state is a particular case: Here, the CC2 method was found to substantially underestimate the excitation energy, with a deviation of about 1 eV from the EOM-CCSD result. A possible reason for this poor agreement is the more complicated electronic structure of the $n_{\text{Ph}}-\pi_1^*$ state and, in particular, the somewhat higher weight of doubly excited configurations as compared to the other states. In view of this, the transition energy for the $n_{\text{Ph}}-\pi_1^*$ state was adjusted for all systems shown in Figure 2; that is, the transition energy was increased by 0.69 eV to adjust the difference between the $\pi-\pi_1^*$ and $n_{\text{Ph}}-\pi_1^*$ excitation energies to the value obtained from the EOM-CCSD calculation (see table SM2 and discussion above).

A comparison of our present findings with results from the literature is possible only for *p*CTM and *p*CTM[−] (see table SM3 in the Supporting Information). The *p*CTM excitation energies are in close agreement with our previous EOM-CCSD results for *p*-coumaric thio acid as reported in ref 18. As for *p*CTM[−], good agreement is found with previous MS-CASPT2³⁷ and TDDFT³⁸ calculations for the $\pi-\pi_1^*$ and $\pi-\pi_2^*$ states. Regarding the $n_{\text{Ph}}-\pi_1^*$ state, the MS-CASPT2 calculations of ref 37 significantly underestimate its energy, similarly to our CC2 results.

In the following, a detailed discussion of these results will be given. Since the fact that the PYP chromophore is present

(37) Molina, V.; Merchán, M. *Proc. Natl. Acad. Sci. U.S.A.* **2001**, *98*, 4299.(38) Sergi, A.; Grüning, M.; Ferrario, M.; Buda, F. *J. Phys. Chem. B* **2001**, *105*, 4386.

in its deprotonated form plays a central role in the electronic structure properties, we will first comment upon this aspect (section III.A). We subsequently discuss the effect of successively adding amino acid residues as shown in Figure 2 (section III.B). Finally, we summarize our conclusions regarding the appropriate reduced model for the local amino acid environment (section III.C). That the present calculations are indeed representative of the actual native PYP system is confirmed by a fairly good qualitative agreement of our predictions with a number of experimental and theoretical results (see the discussion of section III.C).

A. Role of Deprotonation. Comparison between the neutral ($p\text{CTM}$) and anionic ($p\text{CTM}^-$) chromophores shows that pronounced energetic shifts and reorderings take place as a result of deprotonating the phenolate moiety.

We first address the effect of deprotonation on the $\pi-\pi_1^*$ state, which carries most of the oscillator strength. It is this state which is mainly involved in the photoisomerization process. In the neutral species, this state lies at a much higher energy (4.56 eV) than the absorption maximum of native PYP (2.78 eV); moreover, it is not the lowest excited state, owing to the presence of an $n-\pi_1^*$ state (see also ref 18).

Deprotonation entails a very substantial lowering of the $\pi-\pi_1^*$ state energy, of about 1.7 eV according to our CC2 and EOM-CCSD calculations. This makes the $\pi-\pi_1^*$ state the lowest excited state, with an energy (2.89 eV) close to the PYP absorption maximum (2.78 eV). This prediction is also in good agreement with recent gas-phase experiments on the trans-thiophenyl-*p*-coumarate chromophore whose first absorption maximum is found at 2.70 eV.³⁹

The main reason for the energetic lowering is the substantial increase in energy of the π MO, which lies about 5.6 eV higher than in the protonated species. While the energy of the π_1^* MO also increases, it does so to a lesser extent, by about 3.9 eV.

An alternative explanation for the stabilization of the $\pi-\pi_1^*$ state is based on its charge-transfer character (see the pronounced dipole moment change is given in Table 1). Charge transfer is very favorable in the deprotonated species since the negative charge is partially delocalized in the excited electronic state. (This is in contrast to the ground state, where the negative charge is essentially localized on the phenolic oxygen.)

Another effect of deprotonation is that a new excited state appears, $n_{\text{ph}}-\pi_1^*$, which essentially corresponds to the phenolate lone pair. This state, previously reported by Molina and Merchán,³⁷ is characterized by a relatively low oscillator strength and a very large change of dipole moment (Table 1). Anticipating the discussion in the next sections, this state “disappears” from the set of low-lying excited states because of the effect of the Tyr42 and Glu46 amino acids.

Finally, all excited states of $p\text{CTM}^-$ are auto-ionizing. As can be seen from Figure 2, the lowest ionization threshold of $p\text{CTM}^-$ turns out to fall below the vertical transition energy of the first excited state. Hence, all excited states lie in the ionization continuum, that is, they are resonance states. These states are characterized by a finite life time with respect to electron detachment. Their proper treatment requires special methods, for example, using complex absorbing potentials.⁴⁰

The excited-state autoionization instability of the isolated deprotonated chromophore and its analogues was in fact predicted earlier^{18,41} and is supported by experimental observations.³⁹ As an important effect of the amino acid environment, we anticipate the stabilization of these states by an increase of the IP. This issue is addressed in detail in the next section.

Disregarding the issue of auto-ionization, one can infer upon inspection of Figure 2 that the electronic character of the chromophore in the protein environment remains closer to the isolated anion than to the neutral species. This is supported by experimental observation, in that the absorption wavelength associated with the chromophore's first excited state in the protein environment is very close to that of the isolated anionic chromophore.³⁹ As shown by another recent experimental study,⁴² similar conclusions can be drawn for the green fluorescent protein (GFP) chromophore; note, however, that the chromophore is a neutral species in this case.

B. The Chromophore in Its Local Amino Acid Environment. In the following, we successively address the supermolecular complexes shown in Figure 2. Consideration of this series of systems allows one to identify the effects exerted by the individual amino acids. Three types of effects are expected to be most pronounced: (i) energetic shifts, that is, change of the transition energies, (ii) shifts of the ionization potential, (iii) creation of new electronic states, which reflect the charge redistribution within the supermolecular complex. The series of complexes I to VI (Figure 2) will thus allow us to unravel the combined effects of the protein pocket upon the chromophore.

1. The Chromophore–Arg52 Complex (Complex I). The Arg52 residue has been conjectured to play a decisive role in the stabilization of the chromophore's negative charge, because of its role as a “counterion”, carrying a positively charged guanidium group (see, e.g., refs 4, 15, 39, 41, 43). One would therefore expect at least two of the above mentioned effects to be very pronounced: first, a stabilization with respect to autoionization, by an increase of the ionization potential; second, energetic shifts due to the Coulombic interaction. The first effect is indeed substantial; that is, an almost twofold increase of the first IP is observed (see Figure 2). This makes the lowest excited states stable with respect to autoionization. By contrast, the second effect—a marked energetic stabilization—is apparently absent. As illustrated in Figure 2, only a minor shift of the transition energy occurs in complex I as compared with the isolated anionic chromophore. Explanations for this will be given below. Finally, the third type of effect mentioned above, that is, creation of new electronic states that reflect the charge redistribution in the complex, is indeed observed for complex I (see the discussion below regarding a new charge-transfer state that involves electron migration to the Arg52 residue).

We first turn to the unexpectedly small shifts in transition energies, as illustrated in Figure 2. In particular, the transition energy of the $\pi-\pi_1^*$ state is subject to a slight increase (by 0.12 eV, 14 nm) while the $n_{\text{ph}}-\pi_1^*$ state shows a minor decrease (by 0.09 eV). The weak effect of Arg52 on the $\pi-\pi_1^*$ state is in agreement with a number of experimental observations^{43,44} and with results of the theoretical study of ref 41. Moreover, our

(39) Nielsen, I. B.; Boyé-Péronne, S.; El Ghazaly, M.; Kristensen, M. B.; Brøndsted Nielsen, S.; Andersen, L. H. *Biophys. J.* **2005**, *89*, 2597.

(40) Feuerbacher, S.; Sommerfeld, T.; Cederbaum, L. S. *J. Chem. Phys.* **2004**, *120*, 3201.

(41) He, Z.; Martin, C. H.; Birge, R.; Freed, K. F. *J. Phys. Chem. A* **2000**, *104*, 2939.

(42) Lammich, L.; Petersen, M. A.; Nielsen, M. B.; Andersen, L. H. *Biophys. J.* **2007**, *92*, 201.

prediction of a slight increase of the $\pi-\pi_1^*$ excitation energy seems to be in line with findings for the R52A mutant.⁴³ The authors of that work found that substitution of Arg52 by alanine (Ala) gives rise to a small red shift of the PYP absorption maximum; this could be attributed to the removal of Arg52 (thus decreasing the $\pi-\pi_1^*$ transition energy).

Why are the energetic effects so negligibly small? In fact, the presence of the Arg52 residue does lead to a substantial stabilization of the π MO, by about 2.5 eV. However, the π_1^* and n_{Ph} MOs are stabilized in nearly the same fashion, again by about 2.5 eV. Therefore, the $\pi-\pi_1^*$ and $n_{\text{Ph}}-\pi_1^*$ states experience a stabilization that is nearly equal to the ground state, which implies that practically no change occurs in the transition energies.⁴⁵

Finally, we address what is perhaps the most spectacular effect characterizing complex I: the appearance of a new excited state, $\pi-\text{Arg52}$, which turns out to be the lowest excited state of the complex. This state exhibits an intermolecular charge-transfer character, that is, a substantial amount of electron density has migrated from the chromophore to Arg52. An excited state of similar type was previously identified in the work by Groenhof et al.¹² These authors concluded that the charge-transfer state in question lies very close to the absorption maximum of PYP and should therefore be relevant to the Franck–Condon transition. However, according to our calculations (Table 1), the $\pi-\text{Arg52}$ state has a very small oscillator strength (as a result of the negligible overlap of the π and Arg52 MOs) and can therefore not be responsible for the strong PYP absorption maximum.⁴⁶ More importantly, though, this state is found to shift in energy and eventually “disappear” from the set of lowest excited states as soon as the larger complexes of our series are considered. In particular, addition of the Thr50, Val66, and Tyr98 amino acids, which surround and stabilize the Arg52 residue, leads to the “disappearance” of the $\pi-\text{Arg52}$ state from the set of lowest excited states. One should therefore consider this state as an artifact of the restricted chromophore–Arg52 complex.

Finally, the negligible effect of the Arg52 amino acid on the energetics of the $\pi-\pi_1^*$ state at the Franck–Condon geometry does not exclude a more pronounced influence at other geometries. Thus, the QM/MM study by Groenhof et al. predicts that the Arg52 residue has a very pronounced influence on the S_1-S_0 energy gap at the twisted geometry, and essentially

catalyzes the isomerization process.¹⁵ However, this picture currently remains controversial, both on the experimental⁴⁷ and the theoretical⁴⁸ side.

2. Role of Cys69, Phe62, and Phe96 (Complexes II and III). The Cys69 residue has a special role because it connects the chromophore to the protein pocket. Adding Cys69 (complex II) entails a decrease of the transition energies for the $\pi-\pi_1^*$ and $n_{\text{Ph}}-\pi_1^*$ excited states (by 0.19 and 0.17 eV, respectively), while the energy of the $\pi-\text{Arg52}$ state increases (by 0.15 eV) as compared with the values obtained for the complex I. These changes result in a modified ordering of the excited states, such that the $\pi-\pi_1^*$ state is now the lowest excited state, followed by the $\pi-\text{Arg52}$ and $n_{\text{Ph}}-\pi_1^*$ states (Figure 2).

The stabilization of the $\pi-\pi_1^*$ state (as well as the $n_{\text{Ph}}-\pi_1^*$ state) is very likely related to an enhanced efficiency of transferring negative charge from the phenolic moiety to the alkyl part of the chromophore, as the alkyl part increases in size. Given that the alkyl “tail” is even longer in the protein, the stabilization effect is expected to be even more pronounced. This conjecture is in line with findings of ref 49, which shows that the π and π_1^* natural orbitals feature part of the electron density on the Cys69 fragment.

According to our results for complex III (Figure 2), the Phe62 and Phe96 amino acids have only a minor influence on the excited states under consideration. The transition energies of complex III are almost identical to those found for complex I. One should however note certain changes in the electronic structure of the $\pi-\pi_1^*$ excited state which manifest themselves in a lowering of the oscillator strength and an increase of the dipole moment for that state as compared to the situation in complex I (Table 1). These changes are due to a mixing of the $\pi-\pi_1^*$ state with the other low-lying excited states.

3. Nearest Neighbors of Arg52: Thr50, Val66, and Tyr98 (Complex IV). The Thr50, Val66, and Tyr98 amino acids form hydrogen bonds with Arg52 (complex IV) and are thus expected to have a stabilizing effect on the Arg52 residue. Our results (Figure 2) indeed indicate substantial changes in the set of lowest excited states as compared with complex I. The most noteworthy effect is a considerable increase in energy of the $\pi-\text{Arg52}$ excited state, which now lies outside the energy window we consider (4.8 eV) and thus “disappears” from the set of lowest excited states. The dramatic rise in energy of the $\pi-\text{Arg52}$ state is clearly caused by hydrogen bonds between Arg52 and the group of three neighboring amino acids, resulting in an increase of the Arg52 orbital energy by about 2 eV.

An analysis of the individual effects of the three amino acids leads to the following picture. The Thr50 residue has the strongest influence and leads to an increase of the $\pi-\text{Arg52}$ state energy by about 0.8 eV. The effects of Val66 and Tyr98 are somewhat weaker (with an increase of the $\pi-\text{Arg52}$ state energy by 0.64 and 0.52 eV, respectively). This suggests that the $\pi-\text{Arg52}$ state remains well separated from the lowest excited states even if only one of the three hydrogen bonds is present. This could be relevant for the protein in solution, where certain hydrogen bonds might not be present.⁵⁰

(43) Genick, U. K.; Devanathan, S.; Meyer, T. E.; Canestrelli, I. L.; Williams, E.; Cusanovich, M. A.; Tollin, G.; Getzoff, E. D. *Biochemistry* **1997**, *36*, 8.

(44) Mihara, K.; Hisatomi, O.; Imamoto, Y.; Kataoka, M.; Tokunaga, F. *J. Biochem.* **1997**, *121*, 876.

(45) This situation could possibly change as a function of the position of Arg52 with respect to the chromophore. One would expect that the displacement of the guanidium group towards the phenolic oxygen should stabilize the ground state more than the $\pi-\pi_1^*$ state, since the former has more negative charge on the phenolic oxygen. Conversely, moving the guanidium group towards the alkyl moiety should result in an increased stabilization of the $\pi-\pi_1^*$ state, which is characterized by the increased negative charge on the alkyl part. This implicitly supports the previous conclusion that Arg52 can induce either a blue or a red shift of the absorption maximum, depending on its position.^{4,13,60} Even though Arg52 does not substantially change its location during the chromophore’s isomerization, and starts moving only at a much later step of the photocycle,^{19,61–63} the change in the chromophore’s configuration could entail a change of the relative stabilization of the ground state vs the $\pi-\pi_1^*$ excited state.

(46) One could however conjecture whether the $\pi-\text{Arg52}$ state is indirectly involved in the isomerization process, e.g., via a conical intersection of the potential energy surface (PES) of the $\pi-\text{Arg52}$ state with the optically bright $\pi-\pi_1^*$ state.

(47) Changanet-Barret, P.; Plaza, P.; Martin, M. M.; Chosrowjan, H.; Taniguchi, S.; Mataga, N.; Imamoto, Y.; Kataoka, M. *Chem. Phys. Lett.* **2007**, *434*, 320.

(48) Gromov, E. V.; Burghardt, I.; Hynes, J. T.; Köppel, H.; Cederbaum, L. S. *J. Photochem. Photobiol., A*, in press, 2007.

(49) Mochizuki, Y.; Koikegami, S.; Amari, S.; Segawa, K.; Kitaura, K.; Nakano, T. *Chem. Phys. Lett.* **2005**, *406*, 283.

As far as the transition energies of the $\pi-\pi_1^*$ and $n_{\text{Ph}}-\pi_1^*$ states are concerned, the amino acid triple [Thr50, Val66, Tyr98] exerts only a minor effect. A small lowering of the $\pi-\pi_1^*$ state (by 0.07 eV) and a slight destabilization of the $n_{\text{Ph}}-\pi_1^*$ state is observed. Interestingly, Thr50 by itself entails an energetic increase of both states (~ 0.07 eV for the $\pi-\pi_1^*$ state and ~ 0.09 eV for the $n_{\text{Ph}}-\pi_1^*$ state), while Val66 and Tyr98 result in a lowering of these states. The prediction for Thr50 turns out to be in line with the experimental observations for the T50V mutant.^{44,51,52} The latter studies revealed that substitution of Thr50 by a valine residue gives rise to a red shift of the absorption maximum by 550 cm^{-1} (~ 0.07 eV). This behavior was essentially ascribed to the influence of the hydrogen bonds between the hydroxy group of Thr50 and two other close lying amino acids, Glu42 and Tyr46. Since complex IV does not encompass these latter (see the next section), our results suggest a direct interaction of the Thr50 amino acid with the chromophore. We assume that this interaction involves the hydroxy group of Thr50 and the phenolic oxygen of the chromophore.⁵³

4. Hydrogen Bonds Stabilizing the Phenolate Moiety: Tyr42 and Glu46 (Complex V). The Tyr42 and Glu46 residues have a very strong effect on the low-lying excited states of the chromophore—much stronger than any of the other amino acids. In particular, a considerable increase in energy of the $n_{\text{Ph}}-\pi_1^*$ state is observed. This state is no longer present among the four lowest excited states of complex V, and is expected to lie above 4.40 eV. Such a strong shift is unambiguously due to the hydrogen bonds between the chromophore's phenolic oxygen and the hydroxy groups of Tyr42 and Glu46. The formation of hydrogen bonds is found to result in a substantial decrease in energy (~ 2 eV) of the n_{Ph} (occupied) molecular orbital involved in the $n_{\text{Ph}}-\pi_1^*$ transition. This can be considered the main reason for the increase of the $n_{\text{Ph}}-\pi_1^*$ state energy. The effects of the Tyr42 and Glu46 residues are almost equal (with Tyr42 generating a 0.86 eV increase of the $n_{\text{Ph}}-\pi_1^*$ state, while the effect of Glu46 is stronger by only 0.04 eV).

Formation of hydrogen bonds with the [Tyr42,Glu46] pair also affects the other MOs. In particular, the π , π_2^* , π_1^* , n , and Arg52 MOs (Figure 3) are stabilized by 1.6, 1.0, 0.9, 0.7, and 0.3 eV, respectively. This order reflects to what extent the electron density is located on the phenolic oxygen moiety of the chromophore, thus determining the stabilizing effects of hydrogen bonding. These energy shifts lead to a noticeable change in the transition energies; in particular, an increase of energy of the $\pi-\pi_1^*$ and $\pi-\text{Arg52}$ states is observed (see Figure 2). The energetic rise of the $\pi-\pi_1^*$ state is in agreement with the results of experimental studies of the Y42F and E46Q

mutants.^{44,51,52} These investigations revealed a red shift of the absorption maximum if one of the hydrogen bonds is destroyed, with a red shift of 600 cm^{-1} (~ 0.07 eV) in the case of the Y42F mutant (substitution of Tyr42 by a phenylalanine residue) and a shift of 700 cm^{-1} (~ 0.09 eV) in the case of the E46Q mutant (substitution of Glu46 by a glutamine residue).⁴⁴ Our attempts to model the corresponding hydrogen-bond eliminations by removing either the Tyr42 or Glu46 amino acid fragment from complex V resulted in substantially higher values, that is, 0.27 and 0.30 eV, respectively. These large deviations from experiment are very likely the result of neglecting the new substituents, which replace the native [Tyr42, Glu46] residues.

C. Minimal Model for the Chromophore in Native PYP (Complexes VI and VII). On the basis of the above observations, we now propose a minimal model for the PYP chromophore in its local environment, which includes all of the key effects identified above. This model consists of the $p\text{CTM}^-$ chromophore plus six amino acid fragments (Tyr42, Glu46, Thr50, Arg52, Val66, and Tyr98), here denoted complex VI, and a variant which also comprises the Cys69 fragment (complex VII).

The chromophore in complex VI or VII can be considered as a “specifically stabilized $p\text{CTM}^-$ anion”. Its electronic structure is unambiguously closer to the isolated $p\text{CTM}^-$ anion as compared with the neutral $p\text{CTM}$ species, in that the $\pi-\pi_1^*$ state is the lowest-lying excited state and is well separated from the other states (by more than 1 eV). Further, this state is largely dominated by a single configuration, that is, the $\pi-\pi_1^*$ transition (with a weight of 94%). This is in contrast to the $\pi-\pi_1^*$ state in neutral $p\text{CTM}$ as well as in complexes I to V, which exhibits more complicated electronic structure, with a marked multiconfigurational character. In line with this, the oscillator strength of the $\pi-\pi_1^*$ transition is largest in complexes VI and VII (see Table 1).⁵⁴

In contrast to the isolated $p\text{CTM}^-$ anion, the lowest excited states of complex VI and complex VII are stable with respect to auto-ionization, and the $n_{\text{Ph}}-\pi_1^*$ state is moved to high energies. (For complex VI it is even outside the energy window considered). Likewise, the $\pi-\text{Arg52}$ state is also removed from the relevant energy range. Finally, energetic shifts of the order of 0.5 eV have occurred as compared with the isolated anion.

All of these effects are due to the specific stabilization mechanisms exerted by the surrounding amino acids, as discussed in the preceding sections. In particular, (i) the presence of Arg52 strongly raises the ionization potential, (ii) the two connected groups [Thr50, Val66, Tyr98] and [Tyr42, Glu46] act so as to discard the $n_{\text{Ph}}-\pi_1^*$ and $\pi-\text{Arg52}$ states from the relevant energy window, and (iii) among the latter two groups, the [Tyr42, Glu46] group gives rise to pronounced energetic shifts, owing to hydrogen bonding to the phenolate moiety. (The hydrogen bonding is also expected to bring about a considerable increase (~ 1.5 eV) of the ionization potential of the chromophore). In addition, inclusion of the Cys69 fragment leads to a stabilization of the $\pi-\pi_1^*$ state, in line with our conclusions for complex II. Note that Cys69 also lowers the energy of the $n_{\text{Ph}}-\pi_1^*$ state as mentioned above.⁵⁵

- (50) Düx, P.; Rubinstenn, G.; Vuister, G. W.; Boelens, R.; Mulder, F. A. A.; Härd, K.; Hoff, W. D.; Kroon, A. R.; Crielgaard, W.; Hellingwerf, K. J.; Kaptein, R. *Biochemistry* **1998**, *37*, 12689.
- (51) Mataga, N.; Chosrowjan, H.; Shibata, Y.; Imamoto, Y.; Tokunaga, F. *J. Phys. Chem. B* **2000**, *104*, 5191.
- (52) Brudler, R.; Meyer, T. E.; Genick, U. K.; Devanathan, S.; Woo, T. T.; Millar, D. P.; Gerwert, K.; Cusanovich, M. A.; Tollin, G.; Getzoff, E. D. *Biochemistry* **2000**, *39*, 13478.
- (53) This conjecture is supported by additional calculations for a complex composed of $p\text{CTM}^-$, Arg52, and a modified Thr50 residue, whose hydroxy group was substituted by a hydrogen atom: The energy of the $\pi-\pi_1^*$ state in this complex is by 0.05 eV lower than for the original Thr50 residue. It is thus very likely that a hydrogen bond exists between the phenolic oxygen of the chromophore and the hydroxy group of Thr50. This is furthermore supported by our recent QM/MM calculation where we attempted a full geometry optimization of the chromophore and its local amino acid environment (unpublished results). Note that the hydrogen bond in question was experimentally identified for the Y42F mutant.⁵²

- (54) Although the oscillator strength of the $\pi-\pi_1^*$ transition in complex V is comparable to complexes VI and VII, the low energy of the $\pi-\text{Arg52}$ state in complex V makes it less favorable as a model than complexes VI and VII.

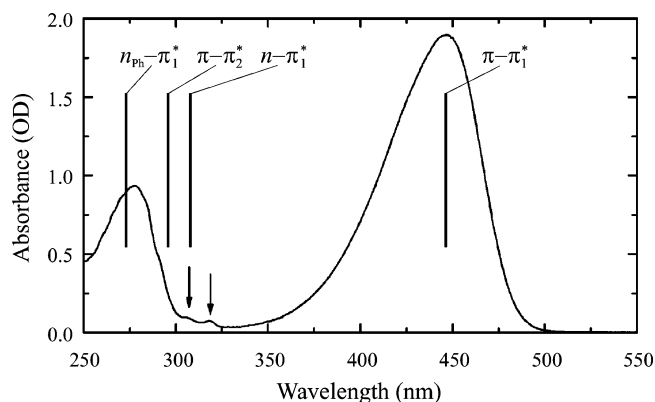


Figure 4. Comparison of the calculated vertical-transition energies for the lowest excited singlet states of complex VII with the experimental absorption spectrum of PYP.⁵⁶ The $\pi-\pi_1^*$ transition was aligned to the maximum of the lowest absorption band, resulting in a red shift of all transition energies by 0.47 eV. The arrows correspond to transitions to the $n-\pi_1^*$ state (experimental assignment).

Our results for complex VII are in qualitative agreement with experimental results, as illustrated in Figure 4. Here, we compare the experimental absorption spectrum by Borucki et al.⁵⁶ with the vertical transition energies for complex VII, indicated by vertical lines. The $\pi-\pi_1^*$ transition was aligned to the maximum of the lowest absorption band (446 nm), thus resulting in a red shift of all transition energies by 0.47 eV (65 nm). The study of ref 56 also addresses the circular dichroism (CD) spectrum of native PYP, and assigns two weak bands at 318 and 307 nm (indicated by arrows in Figure 4) to $n-\pi^*$ transitions, with n referring to a lone pair of the carbonyl oxygen of the chromophore. Our relative energy for the $n-\pi_1^*$ transition is seen to be in very good agreement with the experimental observations. In line with this, the low-energy shoulder (318 nm) very likely corresponds to vibrational progressions, which are expected to be rather extended in the $n-\pi_1^*$ state owing to substantial geometry relaxation effects.¹⁸ There is also another intense band in the absorption spectrum (maximum at ~ 275 nm) which was conjectured to originate in “the aromatic amino acid side chains of PYP with a possible contribution from higher energy transition of the chromophore”.⁵⁶ Our findings for the $\pi-\pi_2^*$ excited state in the complex VII support that prediction. The oscillator strength of the $\pi-\pi_2^*$ transition (calculated for $p\text{CTM}$ and $p\text{CTM}^-$) is the second strongest following the $\pi-\pi_1^*$ transition (Table 1), and should be sufficient for the $\pi-\pi_2^*$ state to be observable in the absorption spectrum of PYP. We therefore suggest that the $\pi-\pi_2^*$ transition contributes to the intensity of the absorption band between 250 and 300 nm (Figure 4).⁵⁷

Overall, a good qualitative agreement with experiment is thus obtained going beyond previous theoretical predictions.^{37,38} A full quantitative agreement is difficult to achieve, in view of errors related to the use of a reduced model system (containing a limited number of amino acids), nonoptimized geometrical

structures, and errors associated with the method and basis set. One might consider including the rest of the protein in a simplified, molecular mechanics (MM) or dielectric continuum description, which could induce additional energetic shifts.

IV. Summary and Conclusions

We have carried out high-level supermolecular calculations, at the CC2 and EOM-CCSD level, in order to identify a reduced model for the PYP chromophore in its native protein environment. To this end, we have considered a series of supermolecular complexes, involving up to 100 atoms, and have identified complex VII as the most accurate reduced representation of the chromophore–environment system. This study prepares the ground for future investigations addressing the influence of the local environment on the isomerization of the PYP chromophore.

By considering the series of complexes I to VII, we have unraveled the diverse influences exerted by the protein environment, all of which act together to produce the unique electronic structure properties of the PYP chromophore. As illustrated very clearly by complex I, electrostatic stabilization of the chromophore–Arg52 “ion-pair” leads to a dramatic increase of the ionization potential, but does not influence the transition energies to any significant extent. The additional charge-transfer state, that is, the LUMO state of complex I, exhibiting an intermolecular electron transfer from the chromophore toward the Arg52 residue, turns out to be an artifact of reducing the environment to the Arg52 residue alone. Further, the hydrogen bonds between the chromophore’s phenolate moiety and the [Tyr42,Glu46] amino acid pair exert the most pronounced energetic shifts, as can be inferred from complex V. Overall, the various stabilization mechanisms combine so as to create a “specifically stabilized $p\text{CTM}^-$ anion”.

Complex VII is the largest supermolecular complex considered in this work, comprising the seven amino acids [Arg52, Cys69, Tyr42, Glu46, Thr50, Val66, Tyr98]. The results obtained for this complex allow one to make predictions which are in qualitative agreement with experimental observations for PYP. The three lowest electronic states of this complex are $\pi-\pi_1^*$, $n-\pi_1^*$, and $\pi-\pi_2^*$ in order of increasing transition energy. While these states appear in a different order than in the isolated $p\text{CTM}^-$ anion, which exhibits the ordering $\pi-\pi_1^*$, $\pi-\pi_2^*$, $n-\pi_1^*$, the electronic character of these states is similar to the anion (and clearly distinct from the neutral $p\text{CTM}$ species). In contrast to the isolated anion, all states are stable with respect to auto-ionization.

The electronic structure of the lowest-lying $\pi-\pi_1^*$ excited state of complex VII, which plays a key role in the chromophore’s isomerization, is remarkably simple in that it is largely dominated by a single configuration. In complexes VI and VII, this state turns out to be well separated from the remaining states, very much like in the isolated anionic $p\text{CTM}^-$

(55) This state was not obtained in complex VI because we evaluated only three lowest excited-state roots. Because of the energy lowering, the $n_{\text{ph}}-\pi_1^*$ state does appear in complex VII, with the energy 4.34 eV. However (see section III), the CC2 method underestimates the energy of this state substantially, and the value obtained was therefore corrected to 5.03 eV (Figure 3). Because of the appearance of the $n_{\text{ph}}-\pi_1^*$ state, the $\pi-\pi_2^*$ state was not explicitly calculated in the complex VII but was extrapolated from the result of complex VI.

(56) Borucki, B.; Otto, H.; Meyer, T. E.; Cusanovich, M. A.; Heyn, M. P. *J. Phys. Chem. B* **2005**, *109*, 629.

(57) We further predict the $n_{\text{ph}}-\pi_1^*$ transition to lie in the relevant energy window. It is however not entirely clear whether it contributes to the intensity of the absorption band under consideration. The oscillator strength of the $n_{\text{ph}}-\pi_1^*$ transition is very small in most of the systems considered (Table 1). This transition can however acquire a certain intensity by the mixing with other excited states, as is the case for complex III (Table 1). Besides, there can be vibronic couplings involving the $n-\pi_1^*$ state, which would likely lead to an intensity borrowing from other states.⁶⁴

species. In contrast to the scenario obtained in ref 58 for the PYP isomerization, involving an S_1 – S_2 barrier, we thus conjecture that a direct isomerization pathway should exist on the S_1 potential surface.

The present investigation prepares the ground for forthcoming work on the dynamics of the isomerization process in the protein environment. The accurate insight obtained from the present *ab initio* perspective is a key ingredient for the correct formulation of reduced dimensionality models. Furthermore, the methodology employed in this study can be transposed to related chromophore–protein systems, for example, various PYP mutants⁵¹ as well as rhodopsin,⁵⁹ the green fluorescent protein,

and their respective mutants. The present approach should therefore contribute to establishing a systematic route to the microscopic study of complex biological photosystems, while providing a valuable benchmark for more approximate methods.

Acknowledgment. Financial support by a DFG/CNRS collaboration project is gratefully acknowledged. We thank Casey Hynes, Pascale Chagnenet-Barret, Monique Martin, and Pascal Plaza for valuable discussions.

Supporting Information Available: Complete refs 34 and 36; discussion of the influence of diffuse functions on the excitation energies; comparison with results of the previous theoretical studies; Cartesian coordinates of geometries discussed in the text. This material is available free of charge via the Internet at <http://pubs.acs.org>.

JA069185L

- (58) Ko, C.; Levine, B.; Toniolo, A.; Manohar, L.; Olsen, S.; Werner, H.-J.; Martínez, T. J. *J. Am. Chem. Soc.* **2003**, *125*, 12710.
- (59) Needleman, R. In *CRC Handbook of Organic Photochemistry and Photobiology*; Horspool, W. M., Song, P., Eds.; CRC Press: Boca Raton, FL, 1995.
- (60) Yoda, M.; Houjou, H.; Inoue, Y.; Sakurai, M. *J. Phys. Chem. B* **2001**, *105*, 9887.
- (61) Genick, U. K.; Borgstahl, G. E. O.; Kingman, N.; Ren, Z.; Pradervand, C.; Burke, P. M.; Šrajcar, V.; Teng, T.-Y.; Schildkamp, W.; McRee, D. E.; Moffat, K.; Getzoff, E. D. *Science* **1997**, *275*, 1471.
- (62) Genick, U. K.; Soltis, S. M.; Kuhn, P.; Canestrelli, I. L.; Getzoff, E. D. *Nature* **1998**, *392*, 206.

- (63) Ren, Z.; Perman, B.; Šrajcar, V.; Teng, T.; Pradervand, C.; Bourgeois, D.; Schotte, F.; Ursby, T.; Kort, R.; Wulff, M.; Moffat, K. *Biochemistry* **2001**, *40*, 13788.
- (64) Köppel, H.; Domcke, W.; Cederbaum, L. S. *Adv. Chem. Phys.* **1984**, *57*, 59.